Theoretical Insights on Methylbenzene Side-Chain Growth in ZSM-5 Zeolites for Methanol-to-Olefin Conversion

ARTICLE *in* CHEMISTRY - A EUROPEAN JOURNAL · SEPTEMBER 2009

Impact Factor: 5.73 · DOI: 10.1002/chem.200901723 · Source: PubMed

5 AUTHORS, INCLUDING:

Michel Waroquier
Ghent University
417 PUBLICATIONS **8,157** CITATIONS

SEE PROFILE

Bryan Marin
Ghent University
400 PUBLICATIONS **4,739** CITATIONS

SEE PROFILE

DOI: 10.1002/chem.200901723

Theoretical Insights on Methylbenzene Side-Chain Growth in ZSM-5 Zeolites for Methanol-to-Olefin Conversion

David Lesthaeghe,*[a] Annelies Horré,[a, b] Michel Waroquier,[a] Guy B. Marin,[c] and Veronique Van Speybroeck*[a]

Abstract: The key step in the conversion of methane to polyolefins is the catalytic conversion of methanol to light olefins. The most recent formulations of a reaction mechanism for this process are based on the idea of a complex hydrocarbon-pool network, in which certain organic species in the zeolite pores are methylated and from which light olefins are eliminated. Two major mechanisms have been proposed to date—the paring mechanism and the side-chain mechanism—recently joined by a third, the alkene mechanism. Recently we succeeded in simulating a full catalytic cycle for the first of these in ZSM-5, with inclusion of the zeolite framework and contents. In this paper, we will investigate crucial reaction steps of the second proposal (the side-chain route) using both small and large zeolite cluster models of ZSM-5. The deprotonation step, which forms an exocyclic double bond, depends crucially on the number and positioning of the other methyl groups but also on steric effects that are typical for the zeolite lattice. Because of steric considerations, we find exocyclic bond formation in the *ortho* position to the geminal methyl group to be more favourable than exocyclic bond formation in the *para* position. The side-chain growth proceeds relatively easily but the major bottleneck is identified as subsequent de-alkylation to produce ethene. These results suggest that the current formulation of the side-chain route in ZSM-5 may actually be a deactivating route to coke precursors rather than an active ethene-producing hydrocarbon-pool route. Other routes may be operating in alternative zeotype materials like the silico-aluminophosphate SAPO-34.

Keywords: density functional calculations · methanol-to-olefins process · methylbenzene · side-chain reactions · zeolites

Introduction

The conversion of methanol to light olefins (methanol-to-olefins, or MTO) is an increasingly important research topic, particularly when one considers the issue of limited oil reserves.[1] Natural gas and coal are needed to fill the void between our current oil-based society and a bio-industry based on renewable resources, which is still in a maturing stage. Both gas and coal can be converted into methanol; MTO technology then provides the key components in the synthesis of many chemicals, amongst which (poly)olefins are the most important.

More than 20 direct mechanisms for the MTO process have been proposed.[1] Recently, through both experimental[2,3] and theoretical studies,[4–6] it became clear that none of these direct mechanisms can lead to the formation of light olefins because of unstable intermediates and activation energies that are too high. The alternative hydrocarbon-pool (HP) proposal states that certain hydrocarbons are stabilised in the pores of the zeolite.[7,8] They undergo successive methylation steps by methanol and/or dimethyl ether and subsequently eliminate light olefins like ethene and propene. The latest experimental findings confirm that the most active of these hydrocarbon-pool species are typically polymethylbenzenes,[9] though linear alkenes may be active HP species as well.[10] The exact nature and reactivity of these polymethylbenzenes is still unclear, however, and is probably highly dependent on zeolite topology.

[a] Dr. D. Lesthaeghe, A. Horré, Prof. Dr. M. Waroquier, Prof. Dr. V. Van Speybroeck
Center for Molecular Modeling
Member of the QCMM Alliance Ghent-Brussels
Ghent University, Proeftuinstraat 86, 9000 Ghent (Belgium)
Fax: (+32) 9264-6697
E-mail: david.lesthaeghe@ugent.be
veronique.vanspeybroeck@ugent.be

[b] A. Horré
Current address: Total Petrochemicals
Scheldelaan 10, 2030 Antwerp (Belgium)

[c] Prof. Dr. G. B. Marin
Laboratorium voor Chemische Technologie
Ghent University, Krijgslaan 281-S5, 9000 Ghent (Belgium)

Experimental and theoretical studies of the HP hypothesis have focussed almost exclusively on two mechanistic ideas: the side-chain and the paring mechanism. A conceptual reaction scheme for both these mechanisms is shown in Scheme 1, though it should be added that only general ideas are shown here and detailed reaction steps are omitted for the sake of clarity. Both mechanisms start with repeated methylation until at some point an already methylated carbon atom is further methylated to form a *gem*-methylated species.[11] Spectroscopic evidence has been given for similar benzenium cations in zeolite H-Beta.[12] In the paring mechanism, such *gem*-methylated species undergo ring contraction that leads to a five-membered ring. After this contraction step, olefins can be eliminated, and the five-membered ring is expanded back to the original six-membered ring. In the side-chain mechanism, on the other hand, although the polymethylbenzene first successively undergoes a *gem*-methylation (just as in the paring mechanism), this is followed by deprotonation to form an exocyclic double bond. This bond is the starting point for side-chain methylation rather than ring methylation, after which elimination of ethene and propene regenerate the original hydrocarbon-pool species.

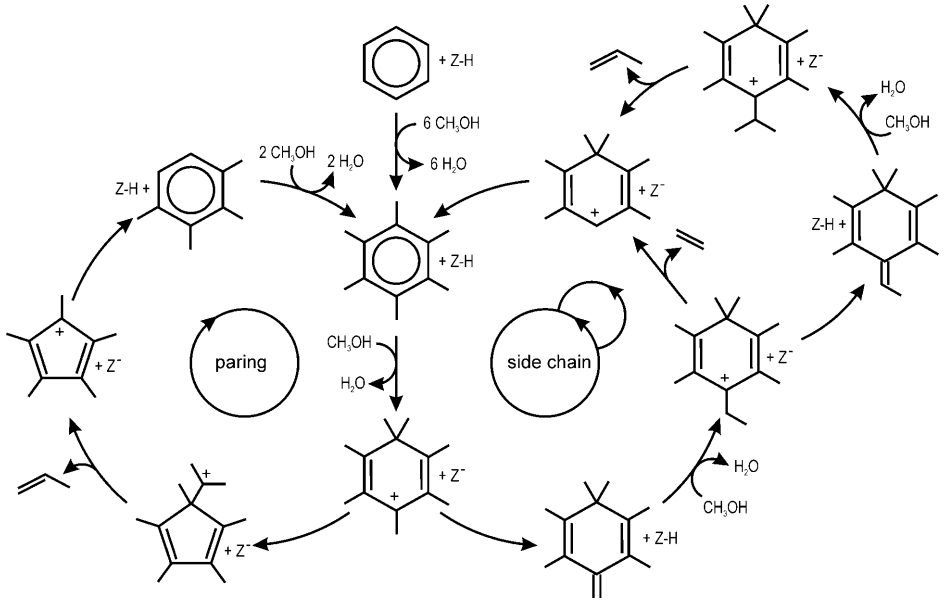

Scheme 1. Schematic representation of the paring and side-chain reaction concepts in MTO catalysis. The zeolite is represented by Z-H or Z^- in its protonated or deprotonated form, respectively.

We have used theoretical methods to gain an understanding of the actual reaction mechanism, which in its turn may then be used to gain control over product distribution. Since the hydrocarbon-pool intermediates are often cationic in nature and quite bulky compared with typical zeolite pore dimensions, the stabilising and steric effects of the zeolite topology must be taken into account in the analysis. We have recently succeeded in simulating a complete reaction path for the paring mechanism in ZSM-5[13] and found that the topology is of utmost importance: some reaction steps become feasible only when the molecular environment is taken into account.[14] For the *gem*-methylation reaction step in particular, our results showed that the reaction rate may vary over seven orders of magnitude depending on the zeolite topology.[11]

In this study, the subsequent reaction steps of the side-chain mechanism are calculated for the ZSM-5 topology. Very recently, the side-chain cycle has been studied in the silico-aluminophosphate H-SAPO-34,[15] with periodic calculations in which hexamethylbenzene is trapped in the small unit cell of the chabazite (CHA) topology. High-energy intermediates were identified for the elimination of ethene and propene. ZSM-5 exhibits different topological limitations and a stronger acid strength, which results in substantial differences in the reaction mechanism for methanol-to-olefin conversion.[9,16] The differences between ZSM-5 and SAPO-34 have been further highlighted recently by the differences in coke formation, as seen through in situ spectroscopy and molecular modelling.[17,18] In the current paper, the full side-chain cycle in ZSM-5 is studied on an extended set of polymethylbenzenes using large cluster calculations that take the topology of ZSM-5 into account, as a comparison to SAPO-34. Conclusions will be drawn on reaction barriers as well as rate coefficients. Since various polymethylbenzenes are studied, our results aim to provide insight into the role of the number and position of methylbenzenes on the reaction rates.

Results and Discussion

We used large, two-layer clusters representing the zeolite framework for the full analysis (see the Computational Methods section), but we will also discuss small pentatetrahedral (5T) cluster results. The use of 5T cluster calculations allows us to separate the effect of zeolite topology from the role of the hydrocarbon-pool species. Some important insights can already be obtained from these smaller calculations on an extensive set of polymethylbenzenes.

Preliminary insights from small 5T cluster calculations: In this section we will concentrate on the first unique step for the side-chain route, that is, deprotonation with the formation of an exocyclic bond, for a whole set of polymethylben-

zenes on the 5T level. The resulting energy barriers will not be representative of the barriers in practice in the zeolite cage (they will be a severe underestimation of the true barrier as discussed in the following paragraph) because of the absence of electrostatic stabilisation of the reactants in particular. However, this approach provides an efficient way to observe certain qualitative trends based on the hydrocarbon-pool intermediate that act independently from the restrictions imposed by the zeolite framework. On the basis of these preliminary insights, a well-defined rationale of hydrocarbon-pool species and active sites is obtained for the subsequent larger cluster calculations in the ZSM-5 topology.

We tested ten different polymethylbenzenes; not only was the number of methyl groups varied but also the position. All the species studied are shown in Scheme 2. Deprotonation was always considered in the *para* position relative to the *gem*-methylated site, as is most commonly suggested in literature.[15]

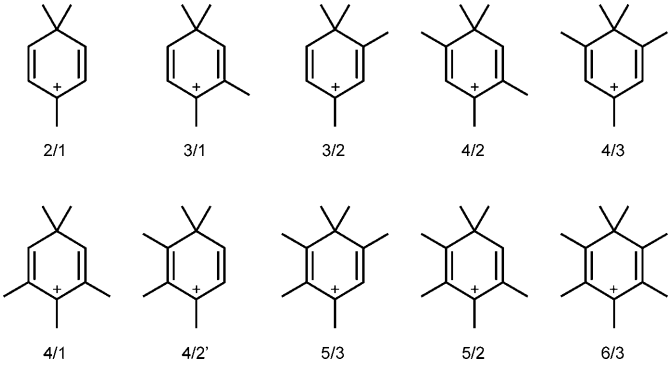

Scheme 2. The set of polymethylbenzenes studied for deprotonation and formation of the exocyclic bond. Each species is labelled *x*/*y*, in which *x* stands for the number of methyl groups on the pre-methylated molecule and *y* for the number of methyl groups in the *ortho* and *para* position relative to the *gem*-methylated site.

As we know from previous work, the higher methylbenzenes form more stable carbenium ions, and thus should be the most difficult to deprotonate.[11] This is in perfect accordance with our observations in Figure 1: the energy barriers increase with increasing number of methyl groups on the aromatic ring, with the heptamethylbenzenium ion (identified by the code 6/3) as the most stable reactant and the most difficult polymethylbenzene to deprotonate (red line in Figure 1). The overall trend that determines the barrier for deprotonation is, however, set by the number of methyl groups in the *ortho*/*para* position, due to the different resonance structures available. Three sets of polymethylbenzenes are clearly segregated: (6/3, 5/3, 4/3), (5/2, 4/2, 4/2′, 3/2) and (4/1, 3/1, 2/1) in order of decreasing barrier for deprotonation. Within each set, the number of methyl groups on the pre-methylated molecule determines the sequence of barriers. Naturally, these two trends are not mutually independent: the higher the methylbenzene, the higher the likelihood of methyl groups in the *ortho*/*para* position and vice

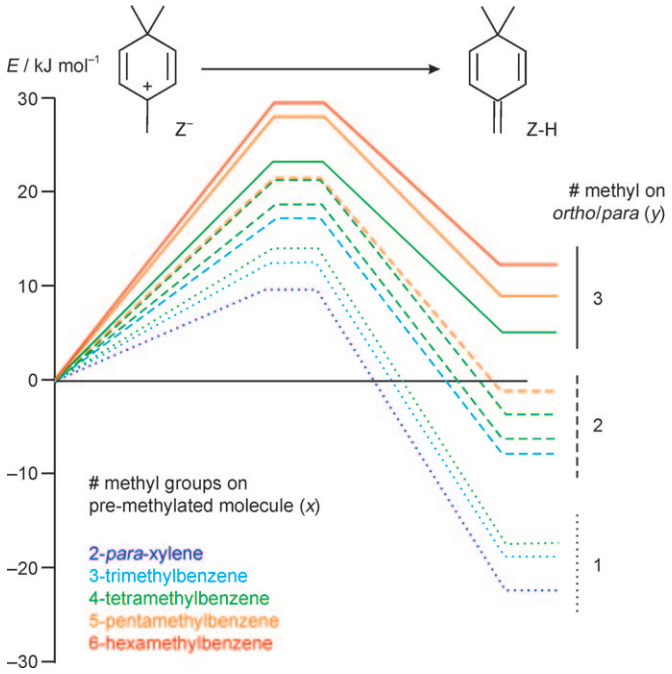

Figure 1. Energy barriers and reaction energy for deprotonation of various *gem*-methylated methylbenzenes obtained from 5T cluster calculations at the B3LYP/6-31+G(d) level of theory. The notation *x*/*y* is defined in Scheme 2.

versa. Nevertheless, the clear separation revealed in Figure 1 shows that the position of the methyl groups on the original hydrocarbon-pool molecule is the primary determinant for the barriers for exocyclic bond formation.

After this over-methylation, the geminal methyl group points towards the active site centred on the aluminium defect as illustrated in Scheme 3. Although in the literature, the *para* position is considered to be the standard deprotonated site, and the *ortho* position is much more likely to be deprotonated from a geometric point of view, since it is much closer to the active site. To deprotonate in the *para* position, as is proposed in Scheme 3, the hydrocarbon-pool molecule would have to rotate almost 180° inside the zeolite

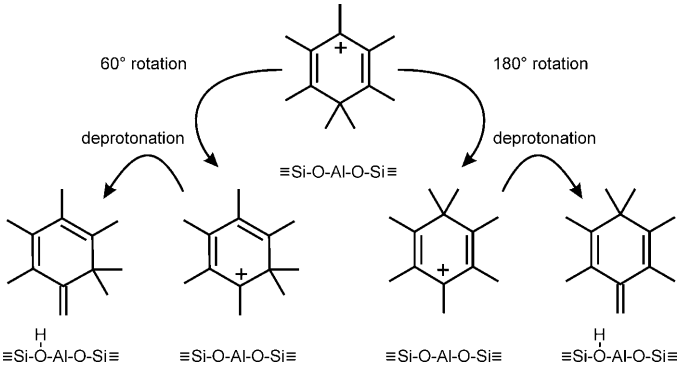

Scheme 3. Orientation of the polymethylbenzene species with respect to the acid proton site in the zeolite.

cage. This is very unlikely in typical MTO catalysts like ZSM-5, for which the space at the channel intersections is very limited.

Beyond the consideration of these geometric implications, one must also know whether there is a large difference energetically between *ortho* and *para* deprotonation. This was examined in detail for 1,1,2,4-tetramethylbenzene (compound 3/2 in Scheme 2) as both deprotonation reactions can be considered on the same compound. Two different starting positions were considered: 1) in which the geminal methyl groups are pointing away from the zeolite active site to deprotonate in the *para* position and 2) in which the geminal methyl groups are pointing towards the active site and the HP species will deprotonate in the *ortho* position relative to the geminal methyl groups. The activation energy and reaction energy are 22.3 and 2.9 kJ mol^{-1} for *ortho* and 17.5 and −7.7 kJ mol^{-1} for *para* deprotonation, respectively. The *ortho* deprotonation is slightly higher in activation energy but the difference in energy barrier is less than 5 kJ mol^{-1} and thus can be considered insignificant compared with the restrictions imposed on starting position and the steric hindrance for rotation in a zeolite cage. Since we will incorporate the zeolite framework limitations in the remainder of this article, we will consider deprotonation in the *ortho* position rather than the *para* position to study the full catalytic side-chain mechanistic cycle. We will use *ortho*-xylene as the starting hydrocarbon-pool species, since this molecule suffers the least from steric limitations; transition-state shape selectivity should thus be held to a minimum.

Note that in the recent paper by Wang et al.[15] who studied this reaction in H-SAPO-34, the issue of excessive rotation was avoided by a computational artefact: by imposing periodic boundary conditions (PBC), the acid site neighbours both sides of the hydrocarbon-pool species simultaneously. This allows the acid site to attack from both the top and the bottom of the molecule. Even though this is an artefact, one could argue that the spacious cages of SAPO-34 allow for more flexibility than the limited space at the channel intersections for ZSM-5 and such a rotation could be considered more likely.

In the following section, we will take these considerations into account and model a full side-chain route in a larger cluster representing the full ZSM-5 catalyst.

Full catalytic side-chain cycle on *ortho*-xylene on ZSM-5

Step 1: gem-*methylation*: The first step of the catalytic cycle is the geminal methylation of a methylbenzene species. This particular reaction step has been studied in detail before, for both small and large clusters, but it is instructive to summarise our main conclusions.[11,13]

1.1) Higher methylbenzenes are more susceptible than lower methylbenzenes to formation of a gem-methyl group: there are more ring carbon atoms on which such an over-methylation might occur and the barriers for methylation are lower.

1.2) The zeolite framework assists in stabilising the carbenium ion product, thus reducing the energy barrier. This reduction is dependent on the size and shape of the cages in each different zeolite topology. In particular we found that the CHA topology of SAPO-34 and SSZ-13 is able to stabilise these cationic species best.

1.3) When there is only limited space, for example, at the channel intersections of ZSM-5, the zeolite framework imposes space limitations on such bulky species, thereby making it harder for the higher methylbenzenes to undergo methylation because of the resulting transition state shape selectivity.

The lower methylbenzenes are, therefore, believed to be the crucial hydrocarbon-pool species in ZSM-5 (as opposed to the higher methylbenzenes in CHA and beta (BEA) topologies). This is in full correspondence with experimental findings.[10]

In the current case, *ortho*-xylene does not suffer from the geometrical constraints found for the larger polymethylbenzene species and the barrier in the large cluster is moderate (115.2 kJ mol^{-1}). Furthermore, as shown earlier in this paper, deprotonation in the *ortho* position with respect to the geminal methyl group will be sterically favoured. The transition state corresponds to a typical, yet slightly distorted S_N2-type geometry. Water is formed and remains connected to the active site by hydrogen bonds, as shown in Figure 2(1).

Step 2: Deprotonation and formation of exocyclic bond: In this reaction step, a proton is transferred from a side methyl group back to the zeolite framework, Figure 2(2). The starting carbenium ion is significantly stabilised by the zeolite framework,[11] which means that the barrier for deprotonation in a full-zeolite surrounding is much higher (139.9 kJ mol^{-1} as shown in Scheme 4) than in the small cluster calculations. The stabilisation effects on the reactants are primarily ascribed to the diffuse electron cloud provided by the framework oxygen atoms.

Step 3: Side-chain growth: To produce olefins in this route, a methylation on the exocyclic bond is required, thereby resulting in a C2 side chain. In full ZSM-5 surroundings, this reaction has a relatively low energy barrier of 99.4 kJ mol^{-1} and is strongly exothermic by −83.1 kJ mol^{-1} (step 3 in Scheme 4). As is the case for step 1, the geometry of the transition state for step 3 also corresponds to an S_N2-type configuration, although significant differences are noticed between this particular ring methylation and side-chain methylation. The carbon–carbon bond that is forming and the carbon–oxygen bond that is breaking are respectively 2.179 and 2.189 Å for the geminal methylation and 2.234 and 1.926 Å for the side-chain methylation. In the case of the ring methylation, the reaction is endothermic (reaction energy of 55.6 kJ mol^{-1}), whereas the side-chain growth is exothermic (reaction energy of −83.1 kJ mol^{-1}), thereby in-

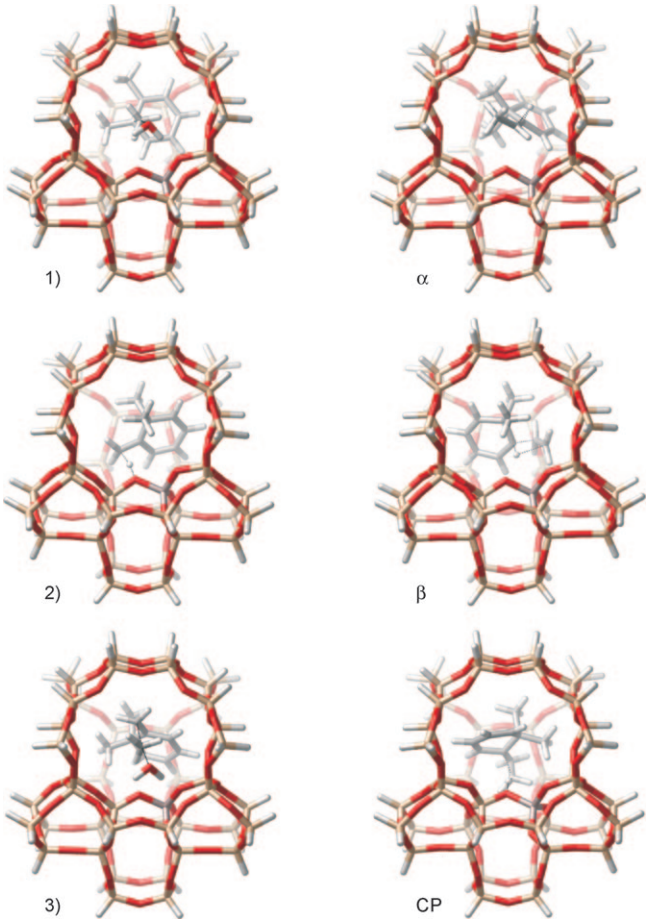

Figure 2. Transition states in the 46T cluster for 1) geminal methylation of *ortho*-xylene, 2) deprotonation with formation of an exocyclic bond, 3) additional methylation with formation of a C2 side chain, and three mechanisms for ethene elimination: α-hydride shift, β-hydride shift, and cyclopropyl (CP) formation.

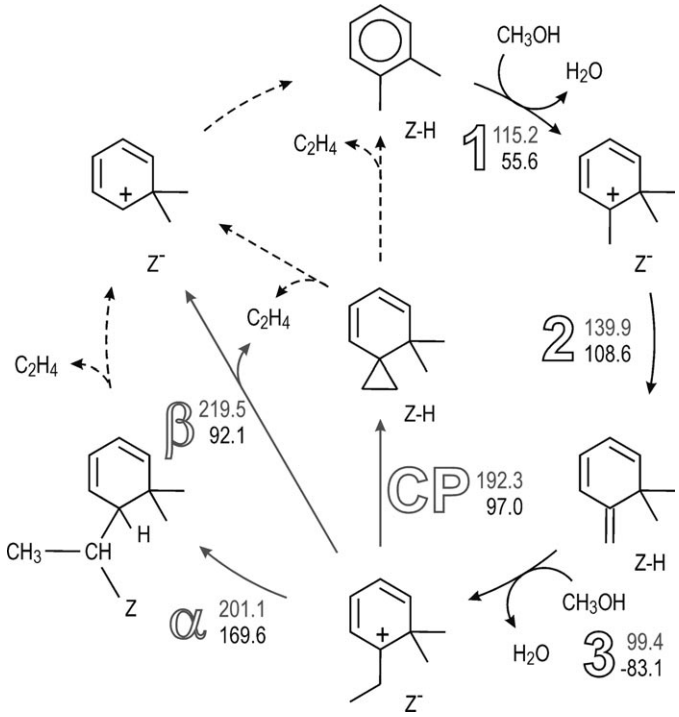

Scheme 4. Full side-chain cycle for the formation of ethene from *ortho*-xylene in ZSM-5. Reaction barriers are shown first, and reaction energies are depicted below. 1) *gem*-Methylation; 2) Deprotonation to exocyclic double bond; 3) Side-chain methylation. Three possible routes provide ethene, from the left inwards: double α-hydride shift, single β-hydride shift, and deprotonation to a cyclopropyl (CP) intermediate.

dicating that the formed carbenium ion is largely stabilised by the framework.

Step 4: Ethene elimination: For the splitting off of ethene, we considered three possible reaction routes. Ethene elimination seems anything but easy: all the reaction barriers hover around 200 kJ mol^{-1}, which is significantly higher than comparable reactions that split off olefins in the paring mechanism.[13] They cannot be considered to indicate viable pathways at typical MTO temperatures.

The three different routes for ethene elimination considered are, from left to right in Scheme 4:

4.1) Two subsequent α-hydride shifts. This reaction path is similar to the elimination of ethene from the cyclopentenyl cation as proposed by Haw et al.[19] Since a tertiary carbenium ion is converted into a secondary carbenium ion, we found this intermediate to be relatively unstable and to exhibit a high energy barrier of 201.1 kJ mol^{-1}. This carbenium ion formed a bond with a basic oxygen atom from the zeolite framework to form a neutral alkoxide species.[20,21] A second hydride shift would split off ethene and a methyl shift would regenerate ortho-xylene, yet these reactions cannot occur if the preceding reaction has an energy barrier that is too high (hence their representation as dashed arrows in Scheme 4).

4.2) With a single β-hydride shift, ethene can be split off immediately. A similar methyl shift and deprotonation would then regenerate the original ortho-xylene hydrocarbon-pool molecule. This barrier too is high, however, as it stands at 219.5 kJ mol^{-1}, and it is unlikely that this reaction would proceed spontaneously under MTO conditions.

4.3) Deprotonation of the side chain forms a spiro structure with a six-membered ring that shares a carbon atom with a three-membered ring. The barrier here is the lowest of the three possibilities investigated, but at 192.3 kJ mol^{-1} it is still high.

In summary, even after investigating three different potential pathways, we find that barriers are systematically around 200 kJ mol^{-1}, and we cannot identify a likely route to ethene formation in ZSM-5. These high barriers also result in low rate coefficients at 673 K, as summarised in Table 1, compared to the paring mechanism.[13] Explicit inclusion of dispersion effects does not noticeably influence these conclusions. We note, furthermore, that this finding is not restricted to this particular zeolite, because a similar conclusion has also been drawn for SAPO-34.[15]

Table 1. Summary of energetics and kinetics for the side-chain catalytic cycle. Forward reaction barriers and rate coefficients at 673 K are shown for both the ONIOM(B3LYP/6-31+G(d):HF/6-31+G(d)//ONIOM-(B3LYP/6-31+G(d):MNDO), shortened as ONIOM, and the B3LYP-D/6-31+G(d) levels of theory.

	ONIOM		B3LYP-D	
	ΔE_0 [kJ mol^{-1}]	k [s^{-1}]	ΔE_0 [kJ mol^{-1}]	k [s^{-1}]
1) *gem*-methylation	115.2	4.80×10^{2}	85.1	1.04×10^{5}
2) deprotonation	139.9	7.97×10^{2}	136.4	1.49×10^{3}
3) side-chain methylation	99.4	2.62×10^{4}	49.2	2.06×10^{8}
α-hydride shift	201.1	1.77×10^{3}	207.4	5.73×10^{4}
β-hydride shift	219.5	8.07×10^{5}	225.1	2.97×10^{5}
CP formation	192.3	2.93×10^{3}	221.6	1.56×10^{5}

Conclusion

The MTO process consists of a complex network of reactions and different hydrocarbon-pool species reacting all at the same time. The side-chain mechanism is a plausible reaction scheme that leads to the formation of ethene, in contrast to the paring mechanism, which mainly forms propene or isobutene. Through theoretical calculations we have found side-chain growth to occur relatively easily in ZSM-5. Noteworthy, however, is that the steric limitations suggest that this side chain is formed in the *ortho* position to the geminal methyl group, rather than the commonly accepted *para* position. The only—but then rather significant—bottlenecks we found were the actual elimination steps of ethene. All energy barriers were too high to be deemed likely routes to ethene formation from methanol.

These results suggest some important practical implications. Since ethene elimination from the side chain is difficult, we believe that this side chain might grow longer, to either split off propene instead, or even to finally lead to deactivation of the catalyst. The facilitation of side-chain growth might, therefore, provide a less active catalyst instead of one that produces more ethene. Other routes to ethene formation certainly require further investigation. Among these, we are currently exploring ethene production by means of the alkene route.

Computational Methods

In a first stage, the zeolite catalyst was modelled by a small 5T cluster for which the B3LYP/6-31+G(d) level of theory was used. The optimised geometries of the HP species and the zeolite active site were then used for more advanced ONIOM (Our owN *n*-layered Integrated molecular Orbital and molecular mechanics Method) calculations. In this research, the MFI topology of ZSM-5 was considered. The level of theory used on these 46T clusters was ONIOM(B3LYP/6-31+G(d):HF/6-31+G(d)//ONIOM(B3LYP/6-31+G(d):MNDO (MNDO = modified neglect of differential overlap), a recipe derived from comparison with full periodic calculations.[22] Saturating hydrogen atoms were kept fixed for geometry optimisations and frequency calculations (PHVA method).[23] To verify the effect of van der Waals interactions we also performed full-cluster single-point B3LYP-D/6-31+G calculations using the Grimme potential.[24,25] These results as well as the corresponding rate coefficients at 673 K are shown in Table 1. It is important to note that although dispersion effects can significantly lower the barrier for the first three steps, they do not do so for the steps that lead to elimination of ethene. Even with inclusion of dispersion effects, these steps are still too slow to be considered viable routes to ethane.

Acknowledgements

This work was supported by the Fund for Scientific Research—Flanders (FWO—Vlaanderen), the Research Board of Ghent University (BOF) and BELSPO, in the framework of the IAP 6/27.

[1] M. Stöcker, *Microporous Mesoporous Mater.* **1999**, *29*, 3.
[2] D. M. Marcus, K. A. McLachlan, M. A. Wildman, J. O. Ehresmann, P. W. Kletnieks, J. F. Haw, *Angew. Chem.* **2006**, *118*, 3205; *Angew. Chem. Int. Ed.* **2006**, *45*, 3133.
[3] W. G. Song, D. M. Marcus, H. Fu, J. O. Ehresmann, J. F. Haw, *J. Am. Chem. Soc.* **2002**, *124*, 3844.
[4] D. Lesthaeghe, V. Van Speybroeck, G. B. Marin, M. Waroquier, *Angew. Chem.* **2006**, *118*, 1746; *Angew. Chem. Int. Ed.* **2006**, *45*, 1714.
[5] D. Lesthaeghe, V. Van Speybroeck, G. B. Marin, M. Waroquier, *Chem. Phys. Lett.* **2006**, *417*, 309.
[6] D. Lesthaeghe, V. Van Speybroeck, G. B. Marin, M. Waroquier, *Ind. Eng. Chem. Res.* **2007**, *46*, 8832.
[7] I. M. Dahl, S. Kolboe, *J. Catal.* **1994**, *149*, 458.
[8] R. M. Dessau, *J. Catal.* **1986**, *99*, 111.
[9] J. F. Haw, W. G. Song, D. M. Marcus, J. B. Nicholas, *Acc. Chem. Res.* **2003**, *36*, 317.
[10] S. Svelle, F. Joensen, J. Nerlov, U. Olsbye, K. P. Lillerud, S. Kolboe, M. Bjorgen, *J. Am. Chem. Soc.* **2006**, *128*, 14770.
[11] D. Lesthaeghe, B. De Sterck, V. Van Speybroeck, G. B. Marin, M. Waroquier, *Angew. Chem.* **2007**, *119*, 1333; *Angew. Chem. Int. Ed.* **2007**, *46*, 1311.
[12] M. Bjorgen, F. Bonino, S. Kolboe, K. P. Lillerud, A. Zecchina, S. Bordiga, *J. Am. Chem. Soc.* **2003**, *125*, 15863.
[13] D. M. McCann, D. Lesthaeghe, P. W. Kletnieks, D. R. Guenther, M. J. Hayman, V. Van Speybroeck, M. Waroquier, J. F. Haw, *Angew. Chem.* **2008**, *120*, 5257; *Angew. Chem. Int. Ed.* **2008**, *47*, 5179.
[14] D. Lesthaeghe, V. Van Speybroeck, M. Waroquier, *Phys. Chem. Chem. Phys.* **2009**, *11*, 5222.
[15] C.-M. Wang, Y.-D. Wang, Z.-K. Xie, Z.-P. Liu, *J. Phys. Chem. C* **2009**, *113*, 4584.
[16] J. F. Haw, *Phys. Chem. Chem. Phys.* **2002**, *4*, 5431.
[17] D. Mores, E. Stavitski, M. H. F. Kox, J. Kornatowski, U. Olsbye, B. M. Weckhuysen, *Chem. Eur. J.* **2008**, *14*, 11320.
[18] K. Hemelsoet, A. Nollet, M. Vandichel, D. Lesthaeghe, V. Van Speybroeck, M. Waroquier, *ChemCatChem* **2009**, in press.
[19] J. F. Haw, J. B. Nicholas, W. G. Song, F. Deng, Z. K. Wang, T. Xu, C. S. Heneghan, *J. Am. Chem. Soc.* **2000**, *122*, 4763.
[20] M. Boronat, P. M. Viruela, A. Corma, *J. Am. Chem. Soc.* **2004**, *126*, 3300.
[21] D. Lesthaeghe, V. Van Speybroeck, M. Waroquier, *J. Am. Chem. Soc.* **2004**, *126*, 9162.
[22] X. Solans-Monfort, M. Sodupe, V. Branchadell, J. Sauer, R. Orlando, P. Ugliengo, *J. Phys. Chem. B* **2005**, *109*, 3539.
[23] A. Ghysels, D. Van Neck, V. Van Speybroeck, T. Verstraelen, M. Waroquier, *J. Chem. Phys.* **2007**, *126*, 13.
[24] S. Grimme, *J. Comput. Chem.* **2006**, 27, 1787.
[25] S. Svelle, C. Tuma, X. Rozanska, T. Kerber, J. Sauer, *J. Am. Chem. Soc.* **2009**, *131*, 816.

Received: June 23, 2009
Published online: September 11, 2009

